electron density, the higher the reduction potential and the faster the reaction. According to the available stability constants[16] the main species present in solution will be $Co^{III}(N_3)_4$ and $Co^{III}(N_3)_6$ for the investigated $[N_3^-]$ range. For instance, the general mechanism outlined in (11) can account in a qualitative way for the observed $[N_3^-]$ dependence, in which k_1 and k_2 involve substitution (anation) followed by inner-sphere electron transfer.

$$Co^{III}(N_3)_4(H_2O)_2^- + N_3^- \overset{K}{\rightleftharpoons} Co^{III}(N_3)_5H_2O^{2-} + H_2O$$

$$Co^{III}(N_3)_4(H_2O)_2^- + HSO_3^-/SO_3^{2-} \xrightarrow{k_1} Co(II) + 4N_3^- + SO_3^- \quad (11)$$

$$Co^{III}(N_3)_5H_2O^{2-} + HSO_3^-/SO_3^{2-} \xrightarrow{k_2} Co(II) + 5N_3 + SO_3^-$$

The rate law for this mechanism under the condition that $1 + K[N_3^-] \approx K[N_3^-]$ is given in (12), from which it follows that k_{obs}

$$k_{obs} = \left(\frac{k_1}{K[N_3^-]} + k_2\right)[S(IV)] \qquad (12)$$

should depend linearly on $[N_3^-]^{-1}$. This is indeed the case for the data in Figure 7, and the intercept of such a plot (k_2) is in good agreement with the limiting rate constant reached at high $[N_3^-]$. Such relationships could further indicate that the less substituted cobalt(III) azide complexes may undergo an inner-sphere redox reaction with sulfite involving the substitution of a coordinated water molecule, whereas the more substituted species may follow an outer-sphere mechanism. However, the limited available data and complexity of the system do not allow a definite assignment of the species involved.

In conclusion, we would like to point at the rather surprising finding of this study that the rate-determining step for sulfite-catalyzed autoxidation of the cobalt(II) azide complexes is the reduction of the cobalt(III) azide complexes by sulfite to produce the sulfite radical SO_3^-. This mechanistic aspect may play an important role in metal-catalyzed autoxidation reactions of sulfur(IV) oxides and account for the catalytic role of species such as Fe(II/III) and Mn(II/III).[7,19]

Acknowledgment. We gratefully acknowledge financial support from the Deutsche Forschungsgemeinschaft, the Commission of the European Communities, and FAPESP (Brasilian Foundation), as well as suggestions and comments from Prof. Eduardo A. Neves (University of Sao Paulo) and Prof. Michael Hoffmann (Caltech, Pasadena, CA).

Registry No. Co, 22541-53-3; N_3, 14343-69-2; SO_3^{2-}, 14265-45-3.

Contribution from the Departments of Chemistry and Medicinal & Biological Chemistry, University of Toledo, Toledo, Ohio 43606

Solid-State ^{31}P NMR and X-ray Crystallographic Studies of Tertiary Phosphines and Their Derivatives

Julian A. Davies,* Sylvain Dutremez, and A. Alan Pinkerton

Received August 21, 1990

High-resolution, solid-state ^{31}P NMR spectra of PPh_3 and its oxide, sulfide, and selenide and PCy_3 and its oxide, sulfide, and selenide are presented and interpreted in terms of reported space group information from X-ray crystallographic studies. The spectra of $Ph_2PCH_2CH_2PPh_2$ and $Ph_2PCH_2PPh_2$ are similarly described. In order to fully interpret the NMR spectra, the X-ray crystal structures of PCy_3 (**1**), $OPCy_3$ (**2**), and $SePCy_3$ (**3**) were determined. Data are as follows: **1**, fw = 280.44, trigonal, $P3_1$, a = 9.893 (2) Å, c = 15.446 (3) Å, V = 1309.2 Å^3, Z = 3, D_x = 1.07 g cm^{-3}, λ(Mo $K\alpha_1$) = 0.70930 Å, μ = 1.4 cm^{-1}, $F(000)$ = 468, T = 294 (1) K, R = 0.045 for 1092 unique reflections with $F^2 > 3\sigma(F^2)$; **2**, fw = 296.44, triclinic, $P\bar{1}$, a = 9.799 (4) Å, b = 16.402 (6) Å, c = 17.067 (6) Å, α = 101.30 (3)°, β = 90.39 (3)°, γ = 99.86 (3)°, V = 2647.8 Å^3, Z = 6, D_x = 1.23 g cm^{-3}, λ(Mo $K\bar{\alpha}$) = 0.71073 Å, μ = 1.6 cm^{-1}, $F(000)$ = 1086, T = 294 (1) K, R = 0.051 for 4939 unique reflections with $F^2 > 3\sigma(F^2)$; **3**, fw = 359.40, orthorhombic, $Pnma$, a = 11.110 (1) Å, b = 15.803 (2) Å, c = 10.364 (1) Å, V = 1819.6 Å^3, Z = 4, D_x = 1.31 g cm^{-3}, λ(Mo $K\bar{\alpha}$) = 0.71073 Å, μ = 21.2 cm^{-1}, $F(000)$ = 760, T = 294 (1) K, R = 0.034 for 1308 unique reflections with $F^2 > 3\sigma(F^2)$.

Introduction

CP/MAS NMR methods[1] provide structural data on solid-phase materials that may serve as an important bridge between high-resolution solution NMR data and information generated by single-crystal X-ray diffraction. In this context, it is important that the differences in these analytical methods, particularly with respect to differentiation of subtle structural changes, be understood.

Data collected by high-resolution solution NMR methods and by CP/MAS solid-state NMR techniques have been compared and contrasted by many workers, and Fyfe[2] has summarized many of the important results. Considering CP/MAS ^{31}P NMR and high-resolution solution ^{31}P or $^{31}P\{^1H\}$ NMR methods as repre-

Table I. Solution and Solid-State ^{31}P NMR Data

compd	soln data:[a] δ(P)/ppm	solid-state data: δ(P)/ppm	compd	soln data:[a] δ(P)/ppm	solid-state data: δ(P)/ppm
PPh_3	−5.31	−7.20	$SPCy_3$	61.92	63.12
$OPPh_3$	29.61	28.99	$SePCy_3$	58.35[d]	60.61[e]
$SPPh_3$	43.36	46.37	dppm	−22.48	−22.33[f]
$SePPh_3$	35.36[b]	37.91[c]			−23.54[f]
PCy_3	11.13	9.28	dppe	−12.59	−9.95
$OPCy_3$	49.84	49.37			
		50.18			

[a] All solution $^{31}P\{^1H\}$ NMR data were measured in $CDCl_3$ at room temperature and referenced to external 85% H_3PO_4. [b] $^1J(^{31}P,^{77}Se)$ = 728 Hz. [c] $^1J(^{31}P,^{77}Se)$ = 737 Hz. [d] $^1J(^{31}P,^{77}Se)$ = 673 Hz. [e] $^1J(^{31}P,^{77}Se)$ = 684 Hz. [f] $^2J(^{31}P,^{31}P)$ = 210 Hz.

---

(1) For an introduction to CP/MAS NMR methods see: (a) Haeberlen, U. *High Resolution NMR in Solids: Selective Averaging*; Academic Press: New York, 1976. (b) Lyerla, J. R. *Contemp. Top. Polym. Sci.* **1979**, *3*, 143. (c) Yannoni, C. S. *Acc. Chem. Res.* **1982**, *15*, 201. (d) Mehring, M. *Principles of High Resolution NMR in Solids*; 2nd ed.; Springer-Verlag: Berlin, 1983. (e) Maciel, G. E. *Science* **1984**, *226*, 282. (f) Harris, R. K. *Analyst* **1985**, *110*, 649. (g) Fyfe, C. A.; Wasylishen, R. E. In *Solid-State Chemistry: Techniques*; Cheetham, A. K., Day, P., Eds.; Clarendon Press: Oxford, England, 1987; pp 190-230.

(2) Fyfe, C. A. *Solid State NMR for Chemists*; C. F. C. Press: Guelph, Ontario, Canada, 1983.

0020-1669/91/1330-2380$02.50/0

sentative examples of the techniques, it is seen that many materials exhibit spectra that show considerable sensitivity to solid-state effects.[3] In particular, many materials exhibit multiple signals in the solid state for each signal observed for a solution sample. The platinum(II) complex *cis*-$[\mathrm{PtCl_2(PPh_3)_2}]$ serves as a typical example. In solution, the $^{31}\mathrm{P}\{^{1}\mathrm{H}\}$ NMR spectrum consists of a single signal with appropriate coupling to ^{195}Pt, but in the solid state, two sets of signals are observed.[3f,w,4]

In order to understand signal multiplicity in solid-state CP/MAS NMR spectra, X-ray crystallography is valuable, since it provides important symmetry information. In the case of *cis*-$[\mathrm{PtCl_2(PPh_3)_2}]$, the X-ray structure (albeit of an acetone solvate) shows that the compound crystallizes in the monoclinic space group $P2_1/c$ with $Z = 4$.[5] Accordingly, the asymmetric unit contains one molecule and hence two unique ^{31}P nuclei. The observation of two signals in the solid-state spectrum is thus in accord with the crystallographic data, and the lack of observable coupling between the inequivalent centers can be rationalized, since $^{2}J(^{31}\mathrm{P},^{31}\mathrm{P})_{cis}$ may be small[6] compared to the solid-state line width.

Harris and co-workers[7] have demonstrated the importance of considering both solid-state NMR data and X-ray crystallographic data together in their studies of diphosphine disulfides. A recent study by Penner and Wasylishen[8] on tertiary phosphines similarly made important comparisons between the techniques but was limited by the restricted availability of X-ray crystallographic data on the compounds considered.

Here we describe the solid-state CP/MAS ^{31}P NMR spectra of two series of tertiary phosphines and their derivatives and examine the results in terms of X-ray crystallographic data. As part of this study, it was necessary to obtain structural data for tricyclohexylphosphine, tricyclohexylphosphine oxide, and tricyclohexylphosphine selenide. The results of these structure determinations are included here. Of particular interest to us is understanding what condition or conditions might be necessary and sufficient for the observation of multiple resonances in solid-state spectra. Particularly intriguing is the possibility that solid-state NMR methods might be used to detect the presence or absence of symmetry elements in crystalline materials and hence be used to solve space group ambiguity problems in X-ray crystallography. Some of our preliminary results in this area have been presented previously.[9]

Experimental Section

(A) Sample Preparation. $\mathrm{PPh_3}$ was purchased from Aldrich Chemical Co. $\mathrm{PCy_3}$ and $\mathrm{Ph_2PCH_2PPh_2}$ were obtained from Strem Chemicals. $\mathrm{Ph_2PCH_2CH_2PPh_2}$ was a gift from M&T Chemicals, Inc. $\mathrm{OPPh_3}$ and $\mathrm{OPCy_3}$ were prepared by reaction of $\mathrm{PPh_3}$ and $\mathrm{PCy_3}$ with a slight excess of $\mathrm{H_2O_2}$, as previously described.[10] $\mathrm{SPPh_3}$, $\mathrm{SePPh_3}$, $\mathrm{SPCy_3}$, and $\mathrm{SePCy_3}$ were prepared by reaction of $\mathrm{PPh_3}$ and $\mathrm{PCy_3}$ with elemental sulfur or selenium according to literature methods.[11] All reactions involving sulfur and selenium were conducted under an inert atmosphere of nitrogen and with dry deoxygenated benzene as a solvent.

(B) NMR Spectra. The solution $^{13}\mathrm{C}\{^{1}\mathrm{H}\}$ NMR spectra were recorded at 100.6 MHz on a Varian VXR-400 spectrometer and referenced to internal $\mathrm{SiMe_4}$. The solution $^{31}\mathrm{P}\{^{1}\mathrm{H}\}$ NMR spectra were recorded on a JEOL FX-90Q spectrometer operating in the FT mode at 36.20 MHz and were referenced to external 85% $\mathrm{H_3PO_4}$, positive shifts representing deshielding. Cross-polarization magic angle spinning (CP/MAS) $^{13}\mathrm{C}\{^{1}\mathrm{H}\}$ and $^{31}\mathrm{P}\{^{1}\mathrm{H}\}$ NMR spectra were obtained on a Chemagnetics CMC-200 medium-bore (70-mm) spectrometer operating at 4.7 T (^{13}C at 50 MHz and ^{31}P at 81 MHz) using high-power proton-decoupling. A 2.5-kHz sweep width and a recycle delay time of 60 s were used in the ^{13}C CP/MAS experiments. A 20-kHz sweep width and a recycle delay time of 6–10 s were employed in the ^{31}P CP/MAS experiments. Between 200 and 300 mg of sample was spun at 3.5–4.7 kHz in zirconia rotors. Carbon chemical shifts were referenced to the aliphatic carbon signal of hexamethylbenzene ($\delta = 17.3$ ppm),[12] while phosphorus chemical shifts were referenced to an external sample of $\mathrm{PPh_3}$ ($\delta = -7.2$ ppm).[3f] The uncertainties in chemical shifts and coupling constants are estimated to be ±0.4 ppm and ±20 Hz, respectively, for the CP/MAS measurements. The "magic angle" of 54° 44′ was set experimentally by optimizing the sideband pattern of the ^{79}Br resonance obtained for a sample of KBr as previously described by Frye and Maciel.[13] Each spectrum was run at two different spinning speeds in order to identify isotropic chemical shifts.

(C) Crystal Structure Analyses. Crystals of $\mathrm{PCy_3}$ suitable for X-ray crystal structure determination were obtained via vacuum sublimation

---

(3) (a) Diesveld, J. W.; Menger, E. M.; Edzes, H. T.; Veeman, W. S. *J. Am. Chem. Soc.* **1980**, *102*, 7935. (b) Maciel, G. E.; O'Donnell, D. J.; Greaves, R. In *Catalytic Aspects of Metal Phosphine Complexes*; Joint Conference CIC and ACS: Guelph, Ontario, Canada, 1980. (c) Maciel, G. E.; O'Donnell, D. J.; Greaves, R. In *Catalytic Aspects of Metal Phosphine Complexes*; Alyea, E. C., Meek, D. W., Eds.; ACS Symposium Series 196; American Chemical Society: Washington, DC, 1982; pp 389–408. (d) Dennis, L. W.; Bartuska, V. J.; Maciel, G. E. *J. Am. Chem. Soc.* **1982**, *104*, 230. (e) Bemi, L.; Clark, H. C.; Davies, J. A.; Drexler, D.; Fyfe, C. A.; Wasylishen, R. *J. Organomet. Chem.* **1982**, *224*, C5. (f) Bemi, L.; Clark, H. C.; Davies, J. A.; Fyfe, C. A.; Wasylishen, R. E. *J. Am. Chem. Soc.* **1982**, *104*, 438. (g) Fyfe, C. A.; Bemi, L.; Clark, H. C.; Davies, J. A.; Gobbi, G. C.; Hartman, J. S.; Hayes, P. J.; Wasylishen, R. E. In *Inorganic Chemistry: Toward the 21st Century*; Chisholm, M. H., Ed.; ACS Symposium Series 211; American Chemical Society: Washington, DC, 1983; pp 405–430. (h) Clark, H. C.; Davies, J. A.; Fyfe, C. A.; Hayes, P. J.; Wasylishen, R. E. *Organometallics* **1983**, *2*, 177. (i) Fyfe, C. A.; Clark, H. C.; Davies, J. A.; Hayes, P. J.; Wasylishen, R. E. *J. Am. Chem. Soc.* **1983**, *105*, 6577. (j) Kroto, H. W.; Klein, S. I.; Meidine, M. F.; Nixon, J. F.; Harris, R. K.; Packer, K. J.; Reams, P. *J. Organomet. Chem.* **1985**, *280*, 281. (k) Allman, T.; Lenkinski, R. E. *Inorg. Chem.* **1986**, *25*, 3202. (l) Komoroski, R. A.; Magistro, A. J.; Nicholas, P. P. *Inorg. Chem.* **1986**, *25*, 3917. (m) Kumar, K. R.; Choudary, B. M.; Moroz, B.; Mastikhin, V. M.; Likholobov, V. A. *J. Mol. Catal.* **1987**, *40*, 327. (n) Clark, H. C.; Fyfe, C. A.; Hayes, P. J.; McMahon, I.; Davies, J. A.; Wasylishen, R. E. *J. Organomet. Chem.* **1987**, *322*, 393. (o) Nelson, J. H.; Rahn, J. A.; Bearden, W. H. *Inorg. Chem.* **1987**, *26*, 2192. (p) Harris, R. K.; Wilkes, P. J.; Wood, P. T.; Woollins, J. D. *J. Chem. Soc., Dalton Trans.* **1989**, 809. (q) Benn, R.; Mynott, R.; Topalović, I.; Scott, F. *Organometallics* **1989**, *8*, 2299. (r) Randall, L. H.; Carty, A. J. *Inorg. Chem.* **1989**, *28*, 1194. (s) Rahn, J. A.; O'Donnell, D. J.; Palmer, A. R.; Nelson, J. H. *Ibid.* **1989**, *28*, 2631. (t) Carty, A. J.; Fyfe, C. A.; Lettinga, M.; Johnson, S.; Randall, L. H. *Ibid.* **1989**, *28*, 4120. (u) Taqui Khan, M. M.; Siddiqui, M. R. H.; Samad, S. A. *Ibid.* **1989**, *28*, 4427. (v) Attar, S.; Bearden, W. H.; Alcock, N. W.; Alyea, E. C.; Nelson, J. H. *Ibid.* **1990**, *29*, 425. (w) Rahn, J. A.; Baltusis, L.; Nelson, J. H. *Ibid.* **1990**, *29*, 750. (x) Bowmaker, G. A.; Cotton, J. D.; Healy, P. C.; Kildea, J. D.; Bin Silong, S.; Skelton, B. W.; White, A. H. *Inorg. Chem.* **1989**, *28*, 1462. (y) Bowmaker, G. A.; Camus, A.; Healy, P. C.; Skelton, B. W.; White, A. H. *Inorg. Chem.* **1989**, *28*, 3883. (z) Robert, J. B.; Wiesenfeld, L. *Mol. Phys.* **1981**, *44*, 319.

(4) Note that the $^{31}\mathrm{P}\{^{1}\mathrm{H}\}$ CP/MAS data reported for *cis*-$[\mathrm{PtCl_2(PPh_3)_2}]$ in ref 3f are significantly different from those reported in ref 3w. The chemical shifts and $^{1}J(^{195}\mathrm{Pt},^{31}\mathrm{P})$ coupling constants reported for *cis*-$[\mathrm{PtCl_2(PPh_3)_2}]$ in ref 3f are 12.9 ppm (3877 Hz) and 8.6 ppm (3623 Hz), whereas those reported in ref 3w are 7.9 ppm (3625 Hz) and −4.1 ppm (3421 Hz). It was suggested in ref 3w that this difference might be due to "environmental effects". However, the $^{31}\mathrm{P}\{^{1}\mathrm{H}\}$ solution NMR data reported for the sample analyzed in ref 3w, i.e. $\delta = -7.8$ ppm and $^{1}J(^{195}\mathrm{Pt},^{31}\mathrm{P}) = 3551$ Hz, are not those of *cis*-$[\mathrm{PtCl_2(PPh_3)_2}]$. The correct $^{31}\mathrm{P}\{^{1}\mathrm{H}\}$ solution NMR data for *cis*-$[\mathrm{PtCl_2(PPh_3)_2}]$ are those indicated in ref 3f, i.e. $\delta = 14.3$ ppm and $^{1}J(^{195}\mathrm{Pt},^{31}\mathrm{P}) = 3673$ Hz. An anonymous reviewer has kindly provided us with copies of the original data collected for the sample reported in ref 3w. It seems that the solution NMR data were incorrectly cited in this report and the actual data ($\delta = 14.3$ ppm and $^{1}J(^{195}\mathrm{Pt},^{31}\mathrm{P}) = 3672$ Hz) are in good agreement with those cited in ref 3f. Nonetheless, the solid-state NMR data described in refs 3f and 3w are strikingly different. Interestingly, a third report on *cis*-$[\mathrm{PtCl_2(PPh_3)_2}]$ has appeared and the solid-state NMR data ($\delta_1 = 7.8$ ppm, $^{1}J(^{195}\mathrm{Pt},^{31}\mathrm{P}) = 3580$ Hz and $\delta_2 = 12.6$ ppm, $^{1}J(^{195}\mathrm{Pt},^{31}\mathrm{P}) = 3750$ Hz) agree well with those reported in ref 3f; see: Allman, T. *J. Magn. Reson.* **1989**, *83*, 637.

(5) Anderson, G. K.; Clark, H. C.; Davies, J. A.; Ferguson, G.; Parvez, M. *J. Crystallogr. Spectrosc. Res.* **1982**, *12*, 449.

(6) (a) Davies, J. A. In *The Chemistry of the Metal-Carbon Bond*; Hartley, F. R., Patai, S., Eds.; John Wiley and Sons: Chichester, England, 1982; Vol. 1, pp 813–918. (b) Pregosin, P. S.; Kunz, R. W. In *NMR, Basic Principles and Progress, Vol. 16: ^{31}P and ^{13}C NMR of Transition Metal Phosphine Complexes*; Diehl, P., Fluck, E., Kosfeld, R., Eds.; Springer-Verlag: Berlin, 1979.

(7) Harris, R. K.; Merwin, L. H.; Hägele, G. *J. Chem. Soc., Faraday Trans. 1* **1987**, *83*, 1055.

(8) Penner, G. H.; Wasylishen, R. E. *Can. J. Chem.* **1989**, *67*, 1909.

(9) Dutremez, S.; Davies, J. A.; Nar, H.; Pinkerton, A. A.; Stieneker, A. Investigation of Space Group Ambiguity in Tris(dithiophosphinato) Complexes Using ^{31}P MAS NMR. Presented at the ACA Annual Meeting, Philadelphia, PA, June 1988; abstract No. PH13.

(10) Hays, H. R. *J. Org. Chem.* **1966**, *31*, 3817.

(11) Bartlett, P. D.; Meguerian, G. *J. Am. Chem. Soc.* **1956**, *78*, 3710.

(12) System Operation Manual for VXR-Series NMR Spectrometer Systems. Publication No. 87-178214-00, Rev. B0186, August 21, 1986, Chapter 20, p 25.

(13) Frye, J. S.; Maciel, G. E. *J. Magn. Reson.* **1982**, *48*, 125.

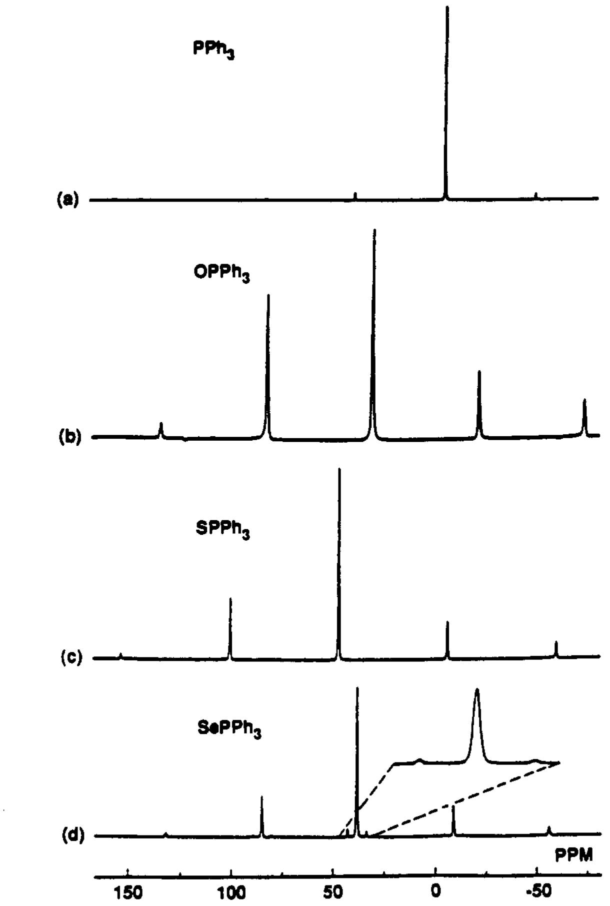

Figure 1. Solid-state ^{31}P NMR spectra: (a) PPh$_3$, 1154 transients, 0 Hz line broadening, spinning rate = 3.5 kHz; (b) OPPh$_3$, 3031 transients, 0 Hz line broadening, spinning rate = 4.2 kHz; (c) SPPh$_3$, 3918 transients, 0 Hz line broadening, spinning rate = 4.3 kHz; (d) SePPh$_3$, 4526 transients, 0 Hz line broadening, spinning rate = 3.8 kHz.

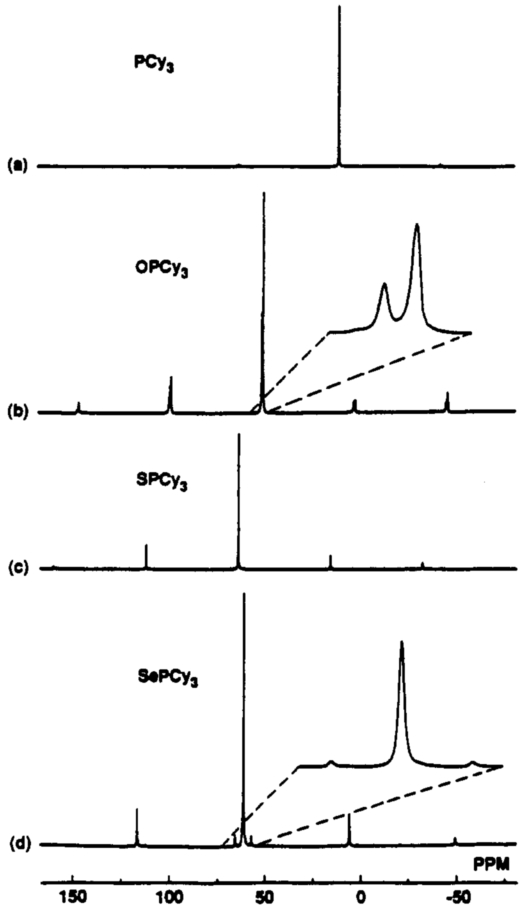

Figure 2. Solid-state ^{31}P NMR spectra: (a) PCy$_3$, 4803 transients, 0 Hz line broadening, spinning rate = 4.3 kHz; (b) OPCy$_3$, 12056 transients, 0 Hz line broadening, spinning rate = 3.9 kHz; (c) SPCy$_3$, 10464 transients, 0 Hz line broadening, spinning rate = 3.9 kHz; (d) SePCy$_3$, 6889 transients, 0 Hz line broadening, spinning rate = 4.5 kHz.

(see Results and Discussion). Colorless crystals of OPCy$_3$ were isolated from toluene. Suitable crystals of SePCy$_3$ were grown from hexanes at −2 °C. Crystal data and additional details of data collection and refinement are given in Table II. Preliminary examination and data collection were performed with Mo Kα radiation on an Enraf-Nonius CAD4 computer-controlled κ-axis diffractometer equipped with a graphite crystal, incident-beam monochromator. The data were collected to $2\theta = 52°$ at a temperature of 21 ± 1 °C by using the ω-scan technique for PCy$_3$ and the ω–2θ scan technique for OPCy$_3$ and SePCy$_3$. Octants collected are as follows. 1: h, 0 to 12; k, −12 to 12; l, −19 to 19. 2: h, 0 to 12; k, −20 to 20; l, −21 to 21. 3: h, 0 to 12; k, 0 to 13; l, 0 to 19. In each case, the data were corrected for Lorentz and polarization effects and an empirical absorption correction was applied. An anisotropic decay correction was also made to account for changes in crystal quality during data collection. In all three cases, the structures were solved by direct methods with MULTAN and the remaining atoms located in succeeding difference Fourier syntheses. Anisotropic temperature factors were used for all non-hydrogen atoms. Hydrogen atoms were included in the refinements but restrained to ride on the atom to which they were bonded. The structures were refined in full-matrix least squares where the function minimized was $\sum w(|F_o|-|F_c|)^2$ in which the weight w was defined as $4F_o^2/\sigma^2(F_o^2)$. Scattering factors were taken from Cromer and Waber,[14] and anomalous dispersion effects were included in F_c. All calculations concerning PCy$_3$ were performed on a VAXstation 3100 computer using MOLEN, and those concerning OPCy$_3$ and SePCy$_3$, on a VAX 11/750 computer using SDP/VAX. Systematic absences of $00l$, $l = 3n + 1$, indicated trigonal space group $P3_1$ or $P3_2$ for PCy$_3$. The result is reported here in space group $P3_1$ (No. 144); however, this is not uniquely defined. The final cycle of refinement included 204 variable parameters and converged (largest parameter shift was 0.01 times its esd) with unweighted and weighted agreement factors of 0.045 and 0.051, respectively. The highest peak in the final difference Fourier had a height of 0.28 e/Å^3, and the minimum negative peak had a height of −0.13 e/Å^3. Systematic absences of $hk0$, $h = 2n + 1$, and $0kl$, $k + l = 2n + 1$, indicated orthorhombic space group $Pnma$ or $Pn2_1a$ for SePCy$_3$. The data are reported here in space group $Pnma$ (No. 62) as confirmed by successful refinement. The final cycle of least squares included 97 variable parameters and converged (largest parameter shift was 0.01 times its esd) with unweighted and weighted agreement factors of 0.034 and 0.048, respectively. The highest peak in the final difference Fourier had a height of 0.37 e/Å^3, and the minimum negative peak had a height of −0.29 e/Å^3. There were no systematic absences in the case of OPCy$_3$; the space group was determined to be $P\bar{1}$ (No. 2). The final cycle of refinement included 541 variable parameters and converged (largest parameter shift was 0.01 times its esd) with unweighted and weighted agreement factors of 0.051 and 0.063, respectively. The highest peak in the final difference Fourier had a height of 0.34 e/Å^3, and the minimum negative peak had a height of −0.21 e/Å^3. Final atomic coordinates and equivalent isotropic displacement parameters for PCy$_3$, OPCy$_3$, and SePCy$_3$ are given in Tables III, V, and VII, and selected bond lengths and angles, in Tables IV, VI, and VIII, respectively.

Results and Discussion

Shown in Figure 1 are the solid-state CP/MAS ^{31}P NMR spectra of triphenylphosphine and its oxide, sulfide, and selenide. Like the solid-state spectra shown here, the high-resolution solution $^{31}\mathrm{P}\{^1\mathrm{H}\}$ NMR spectra of these compounds also each exhibit only a single signal, with the selenide showing the expected satellites due to ^{31}P–^{77}Se coupling. Thus, for this family of four compounds, the solid-state and solution spectra each exhibit single signals with good agreement in chemical shifts (Table I) and, for the selenide, coupling constants. The situation is quite different for the analogous series of tricyclohexylphosphine derivatives. Figure 2 shows the solid-state ^{31}P NMR spectra of the parent compound and its oxide, sulfide, and selenide. Although the high-resolution solution $^{31}\mathrm{P}\{^1\mathrm{H}\}$ NMR spectra of each of these compounds show single resonances (Table I), the solid-state spectrum of the oxide

---

(14) Cromer, D. T.; Waber, J. T. *International Tables for X-ray Crystallography*; The Kynoch Press: Birmingham, England, 1974; Vol. IV, Table 2.2B.

Table II. Crystal Data

compd	PCy_3 (**1**)	$OPCy_3$ (**2**)	$SePCy_3$ (**3**)
fw	280.44	296.44	359.40
space group	$P3_1$ (No. 144)	$P\bar{1}$ (No. 2)	*Pnma* (No. 62)
a/Å	9.893 (2)	9.799 (4)	11.110 (1)
b/Å		16.402 (6)	15.803 (2)
c/Å	15.446 (3)	17.067 (6)	10.364 (1)
α/deg		101.30 (3)	
β/deg		90.39 (3)	
γ/deg		99.86 (3)	
V/Å^3	1309.2	2647.8	1819.6
Z	3	6	4
λ/Å	0.70930	0.71073	0.71073
D_x/g cm^{-3}	1.07	1.23	1.31
μ/cm^{-1}	1.4	1.6	21.2
R	0.045	0.051	0.034
R_w	0.051	0.063	0.048

shows two signals, appearing in an approximately 2:1 intensity ratio, thus differing significantly from the spectra of the parent phosphine, the sulfide, and the selenide, each of which exhibit a single signal in the solid state. In addition, Figures 1 and 2 show that the significant differences in chemical shift anisotropies of the phosphines and their oxides, sulfides, and selenides are manifested in the intensities of the spinning sidebands. For example, Figure 1 shows that the intensities of the spinning sidebands decrease in the order $OPPh_3 > SPPh_3 > SePPh_3 > PPh_3$ exactly matching the order of the magnitudes of the chemcial shift anisotropies of these compounds obtained by ^{31}P NMR measurements on static samples.[3z]

For triphenylphosphine, both solution and solid-state measurements produce single resonances. The reported solid-state structure of triphenylphosphine is in the monoclinic space group $P2_1/a$ with $Z = 4$.[15] Thus, the asymmetric unit contains one PPh_3 moiety and, hence, one ^{31}P nucleus. On the basis of the X-ray crystallographic data, no more than one resonance is anticipated in solid-state NMR measurements and only one resonance is observed. In the case of triphenylphosphine oxide, X-ray crystallographic data are reported for two monoclinic forms and one orthorhombic form. The X-ray crystal structures of the two monoclinic forms[16-19] were solved in the space groups $P2_1/a$ and $P2_1/c$ with $Z = 4$, and so we anticipate no more than one ^{31}P resonance in the solid-state NMR spectrum (vide supra) of either polymorph. The remaining polymorph is in the orthorhombic space group *Pbca* with $Z = 8$.[18,20] Here we again find that the asymmetric unit contains a single molecule, and so no more than one resonance should be anticipated in the solid-state ^{31}P NMR spectrum of this polymorph. In our sample we might thus have any one of the three reported polymorphs (or even a mixture of polymorphs with isochronous resonances), since we observe only one signal (Figure 1).

The reported X-ray crystal structures of both triphenylphosphine sulfide[21] and selenide[22] are in the monoclinic space group $P2_1/c$ with $Z = 8$. The asymmetric unit in each structure thus contains two separate molecules and, hence, two distinct ^{31}P nuclei. However, the solid-state ^{31}P NMR spectra reveal only single signals. Thus, we see that crystallographic inequivalence, although obviously necessary, is not sufficient for the observation of separate resonances. Indeed, there is every reason to expect solid-state ^{31}P NMR chemical shifts to exhibit the same structure-sensitivity trends found for solutions, and so two nuclei that are crystallographically inequivalent, but in chemically very similar environments, may be beneath the resolution limit of the NMR experiment. Indeed, although the asymmetric units in Ph_3PS and Ph_3PSe each contain two molecules, the X-ray crystallographic data show that these molecules are nearly identical in both molecular dimensions and conformations.

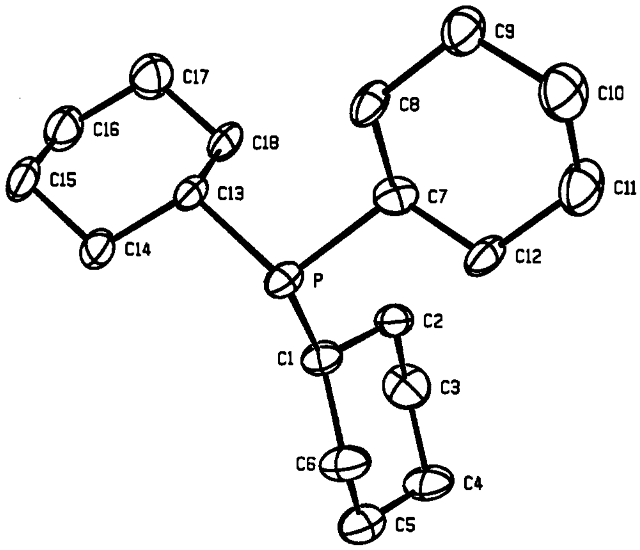

Figure 3. Molecular structure of PCy_3, showing 30% probability ellipsoids.

Table III. Positional Parameters and Equivalent Isotropic Displacement Parameters for PCy_3 (**1**)

atom	x	y	z	B/Å^2 [a]
P	0.2551 (2)	0.1157 (2)	1.000	3.47 (3)
C1	0.2875 (6)	0.2984 (6)	0.9461 (4)	3.9 (2)
C2	0.2250 (7)	0.2891 (6)	0.8559 (4)	4.1 (2)
C3	0.2734 (8)	0.4515 (6)	0.8196 (5)	5.1 (2)
C4	0.2233 (8)	0.5383 (7)	0.8786 (5)	6.1 (2)
C5	0.2814 (8)	0.5491 (7)	0.9692 (5)	5.7 (2)
C6	0.2386 (7)	0.3902 (6)	1.0046 (4)	4.8 (2)
C7	0.0784 (6)	−0.0446 (6)	0.9465 (4)	3.6 (2)
C8	0.0616 (6)	−0.2016 (6)	0.9674 (5)	4.0 (2)
C9	−0.0857 (7)	−0.3340 (7)	0.9282 (5)	5.1 (2)
C10	−0.2322 (7)	−0.3295 (7)	0.9510 (5)	5.5 (2)
C11	−0.2095 (7)	−0.1681 (7)	0.9314 (6)	6.1 (2)
C12	−0.0647 (6)	−0.0392 (6)	0.9730 (5)	4.1 (2)
C13	0.4175 (6)	0.0901 (6)	0.9565 (5)	3.7 (2)
C14	0.5712 (6)	0.2085 (7)	0.9971 (4)	4.5 (2)
C15	0.7040 (6)	0.1772 (7)	0.9713 (5)	5.0 (2)
C16	0.7152 (7)	0.1714 (8)	0.8745 (5)	5.7 (2)
C17	0.5632 (6)	0.0569 (7)	0.8349 (5)	5.4 (2)
C18	0.4359 (6)	0.0880 (7)	0.8598 (4)	4.4 (2)

[a] *B* values for anisotropically refined atoms are given in the form of the isotropic equivalent displacement parameter.

Table IV. Selected Bond Lengths (Å) and Angles (deg) for PCy_3 (**1**)[a]

P–C1	1.867 (6)	C2–C3	1.535 (9)
P–C7	1.865 (5)	C3–C4	1.50 (1)
P–C13	1.871 (7)	C4–C5	1.50 (1)
C1–C2	1.508 (9)	C5–C6	1.511 (9)
C1–C6	1.52 (1)		
C1–P–C7	105.1 (3)	C3–C4–C5	112.7 (7)
C1–P–C13	103.1 (3)	C4–C5–C6	111.5 (5)
C7–P–C13	103.2 (3)	C1–C6–C5	113.5 (5)
P–C1–C2	119.1 (4)	P–C7–C8	110.7 (5)
P–C1–C6	111.2 (4)	P–C7–C12	110.4 (4)
C2–C1–C6	110.0 (6)	P–C13–C14	110.2 (5)
C1–C2–C3	111.7 (5)	P–C13–C18	118.4 (5)
C2–C3–C4	111.0 (6)		

[a] Numbers in parentheses are estimated standard deviations in the least significant digits.

For the tricyclohexylphosphine series, complete X-ray crystallographic data were not available. The X-ray structure of the

---

(15) Daly, J. J. *J. Chem. Soc.* **1964**, 3799.

(16) Gusev, A. I.; Bokii, N. G.; Afonina, N. N.; Timofeeva, T. V.; Kalinin, A. E.; Struchkov, Yu. T. *Zh. Strukt. Khim.* **1973**, *14*, 115; *J. Struct. Chem.* (*Engl. Transl.*) **1973**, *14*, 101.

(17) Ruban, G.; Zabel, V. *Cryst. Struct. Commun.* **1976**, *5*, 671.

(18) Brock, C. P.; Schweizer, W. B.; Dunitz, J. D. *J. Am. Chem. Soc.* **1985**, *107*, 6964.

(19) Spek, A. L. *Acta Crystallogr., Sect. C* **1987**, *43*, 1233.

(20) Bandoli, G.; Bortolozzo, G.; Clemente, D. A.; Croatto, U.; Panattoni, C. *J. Chem. Soc. A* **1970**, 2778.

(21) Codding, P. W.; Kerr, K. A. *Acta Crystallogr., Sect. B* **1978**, *34*, 3785.

(22) Codding, P. W.; Kerr, K. A. *Acta Crystallogr., Sect. B* **1979**, *35*, 1261.

Table V. Positional Parameters and Equivalent Isotropic Displacement Parameters for OPCy$_3$ (**2**)

atom	x	y	z	B/Å^2 [a]
P1	0.42216 (9)	0.42926 (5)	0.24543 (5)	2.95 (2)
P2	0.56203 (9)	0.90514 (5)	−0.33814 (5)	2.87 (2)
P3	0.4250 (1)	0.75585 (5)	0.13374 (5)	3.31 (2)
O1	0.4097 (2)	0.3359 (1)	0.2348 (1)	4.07 (6)
O2	0.5867 (2)	0.9990 (1)	−0.3203 (1)	4.07 (6)
O3	0.4163 (3)	0.6629 (1)	0.1241 (1)	4.49 (6)
C1	0.3637 (3)	0.4727 (2)	0.3441 (2)	3.31 (8)
C2	0.3363 (4)	0.5629 (2)	0.3579 (2)	4.10 (9)
C3	0.3038 (4)	0.5940 (2)	0.4449 (2)	5.2 (1)
C4	0.1859 (4)	0.5360 (2)	0.4712 (2)	5.5 (1)
C5	0.2126 (4)	0.4463 (2)	0.4574 (2)	5.7 (1)
C6	0.2427 (4)	0.4148 (2)	0.3708 (2)	4.80 (9)
C7	0.3273 (3)	0.4619 (2)	0.1687 (2)	3.04 (7)
C8	0.1701 (3)	0.4319 (2)	0.1682 (2)	4.29 (9)
C9	0.0954 (4)	0.4595 (3)	0.1013 (2)	5.2 (1)
C10	0.1500 (4)	0.4278 (2)	0.0208 (2)	5.2 (1)
C11	0.3048 (4)	0.4568 (2)	0.0202 (2)	4.52 (9)
C12	0.3814 (4)	0.4299 (2)	0.0855 (2)	4.00 (9)
C13	0.6028 (3)	0.4772 (2)	0.2402 (2)	3.18 (7)
C14	0.6384 (3)	0.5709 (2)	0.2362 (2)	4.14 (9)
C15	0.7906 (4)	0.5954 (2)	0.2206 (2)	5.4 (1)
C16	0.8847 (4)	0.5752 (2)	0.2817 (2)	5.0 (1)
C17	0.8475 (4)	0.4841 (2)	0.2886 (2)	5.1 (1)
C18	0.6965 (3)	0.4594 (2)	0.3038 (2)	4.62 (9)
C19	0.6485 (3)	0.8629 (2)	−0.2650 (2)	2.96 (7)
C20	0.8052 (3)	0.8928 (2)	−0.2625 (2)	4.18 (9)
C21	0.8786 (4)	0.8610 (3)	−0.1992 (2)	5.4 (1)
C22	0.8243 (4)	0.8881 (3)	−0.1168 (2)	5.2 (1)
C23	0.6693 (4)	0.8594 (2)	−0.1175 (2)	4.41 (9)
C24	0.5930 (4)	0.8890 (2)	−0.1817 (2)	4.02 (9)
C25	0.3771 (3)	0.8640 (2)	−0.3361 (2)	3.03 (7)
C26	0.3311 (3)	0.7688 (2)	−0.3468 (2)	4.15 (9)
C27	0.1763 (4)	0.7449 (2)	−0.3378 (2)	5.0 (1)
C28	0.0941 (4)	0.7789 (2)	−0.3953 (2)	5.1 (1)
C29	0.1367 (4)	0.8734 (2)	−0.3857 (2)	4.9 (1)
C30	0.2918 (4)	0.8986 (2)	−0.3938 (2)	4.51 (9)
C31	0.6170 (3)	0.8633 (2)	−0.4383 (2)	3.16 (7)
C32	0.6476 (4)	0.7733 (2)	−0.4535 (2)	3.73 (8)
C33	0.6752 (4)	0.7433 (2)	−0.5409 (2)	4.8 (1)
C34	0.7897 (4)	0.8025 (2)	−0.5696 (2)	5.5 (1)
C35	0.7624 (4)	0.8919 (2)	−0.5536 (2)	5.4 (1)
C36	0.7340 (4)	0.9229 (2)	−0.4663 (2)	4.61 (9)
C37	0.3337 (3)	0.8000 (2)	0.2197 (2)	3.13 (7)
C38	0.3964 (4)	0.7831 (2)	0.2960 (2)	3.95 (8)
C39	0.3202 (4)	0.8161 (2)	0.3700 (2)	4.29 (9)
C40	0.1665 (4)	0.7831 (3)	0.3611 (2)	5.5 (1)
C41	0.1055 (4)	0.8000 (3)	0.2854 (2)	6.6 (1)
C42	0.1783 (4)	0.7636 (3)	0.2122 (2)	5.3 (1)
C43	0.6053 (4)	0.8097 (2)	0.1510 (2)	4.26 (9)
C44	0.6318 (4)	0.9055 (2)	0.1690 (2)	5.0 (1)
C45	0.7834 (4)	0.9413 (3)	0.1887 (3)	8.1 (1)
C46	0.8805 (4)	0.9063 (3)	0.1306 (3)	6.7 (1)
C47	0.8510 (4)	0.8110 (2)	0.1117 (2)	5.5 (1)
C48	0.7019 (4)	0.7749 (2)	0.0911 (2)	5.5 (1)
C49	0.3608 (4)	0.7841 (2)	0.0443 (2)	5.2 (1)
C50	0.3074 (4)	0.8675 (2)	0.0536 (2)	5.1 (1)
C51	0.2685 (6)	0.8869 (3)	−0.0245 (2)	10.2 (2)
C52	0.1959 (5)	0.8197 (3)	−0.0826 (3)	9.0 (1)
C53	0.2437 (5)	0.7370 (3)	−0.0916 (2)	7.0 (1)
C54	0.2800 (5)	0.7153 (3)	−0.0124 (2)	8.0 (1)

[a] B values for anisotropically refined atoms are given in the form of the isotropic equivalent displacement parameter.

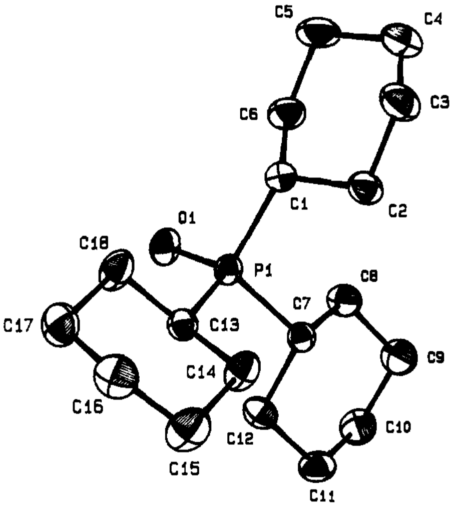

Figure 4. Molecular structure of OPCy$_3$, showing 30% probability ellipsoids.

Table VI. Selected Bond Lengths (Å) and Angles (deg) for OPCy$_3$ (**2**)[a]

P1–O1	1.490 (2)	P2–C25	1.826 (3)
P1–C1	1.831 (3)	P2–C31	1.834 (3)
P1–C7	1.815 (3)	P3–O3	1.488 (2)
P1–C13	1.820 (3)	P3–C37	1.817 (3)
P2–O2	1.487 (2)	P3–C43	1.828 (3)
P2–C19	1.812 (3)	P3–C49	1.818 (4)
O1–P1–C1	110.0 (1)	P1–C1–C2	117.0 (2)
O1–P1–C7	113.5 (1)	P1–C1–C6	113.0 (2)
O1–P1–C13	109.9 (1)	P1–C7–C8	113.4 (2)
C1–P1–C7	109.6 (2)	P1–C7–C12	110.1 (2)
C1–P1–C13	107.6 (1)	P1–C13–C14	119.2 (2)
C7–P1–C13	106.1 (1)	P1–C13–C18	112.9 (2)
O2–P2–C19	112.2 (1)	P2–C19–C20	111.1 (2)
O2–P2–C25	110.0 (1)	P2–C19–C24	110.5 (2)
O2–P2–C31	111.5 (1)	P2–C25–C26	118.1 (2)
C19–P2–C25	106.8 (1)	P2–C25–C30	111.6 (2)
C19–P2–C31	109.3 (1)	P2–C31–C32	116.8 (2)
C25–P2–C31	106.8 (1)	P2–C31–C36	113.0 (2)
O3–P3–C37	112.4 (1)	P3–C37–C38	109.7 (2)
O3–P3–C43	110.5 (2)	P3–C37–C42	112.0 (2)
O3–P3–C49	111.7 (1)	P3–C43–C44	117.4 (3)
C37–P3–C43	105.8 (1)	P3–C43–C48	114.1 (2)
C37–P3–C49	109.6 (2)	P3–C49–C50	118.0 (2)
C43–P3–C49	106.4 (2)	P3–C49–C54	115.5 (3)

[a] Numbers in parentheses are estimated standard deviations in the least significant digits.

sulfide was reported some time ago, and we have solved the structures of the parent phosphine, the oxide, and the selenide.

Several attempts to grow suitable crystals of PCy$_3$ from solvent mixtures failed, and ultimately vacuum sublimation provided us with specimens that proved to be seriously twinned but from which we were able to cut a small, irregular crystal for data collection. Crystal data for PCy$_3$ are collected in Table II, and the molecular structure is shown in Figure 3. The positional parameters and equivalent isotropic displacement parameters are shown in Table III, and selected bond lengths and angles are given in Table IV. The molecular structure of PCy$_3$ is entirely as expected with the cyclohexyl groups adopting chair conformations and the geometry about phosphorus being approximately pyramidal.

We found that PCy$_3$ crystallizes in the trigonal space group $P3_1$ with $Z = 3$, and this explains the serious twinning problems. By considering the contents of the asymmetric unit, we anticipate a single resonance in the solid-state ^{31}P NMR spectrum and this is indeed observed (Figure 2).

Unlike the other spectra shown in Figure 2, that of Cy$_3$PO exhibits two resonances. Given this unusual situation, we felt it worthwhile to solve its X-ray crystal structure also.

Crystal data for Cy$_3$PO are collected in Table II, and the molecular structure is shown in Figure 4. The positional parameters and equivalent isotropic displacement parameters are shown in Table V, and selected bond lengths and angles are given in Table VI. At the molecular level, there is little unusual about the structure of Cy$_3$PO. The cyclohexyl groups adopt the expected chair conformation, and the geometry about phosphorus is approximately tetrahedral. The P1–O1 bond length (1.490 (2) Å) is similar to the P–O bond length in Me$_3$PO (1.489 (6) Å)[23] and

---

(23) Engelhardt, L. M.; Raston, C. L.; Whitaker, C. R.; White, A. H. *Aust. J. Chem.* **1986**, *39*, 2151.

Chart I. Averaged Bond Lengths for Each Molecule in the Unit Cell of $OPCy_3$

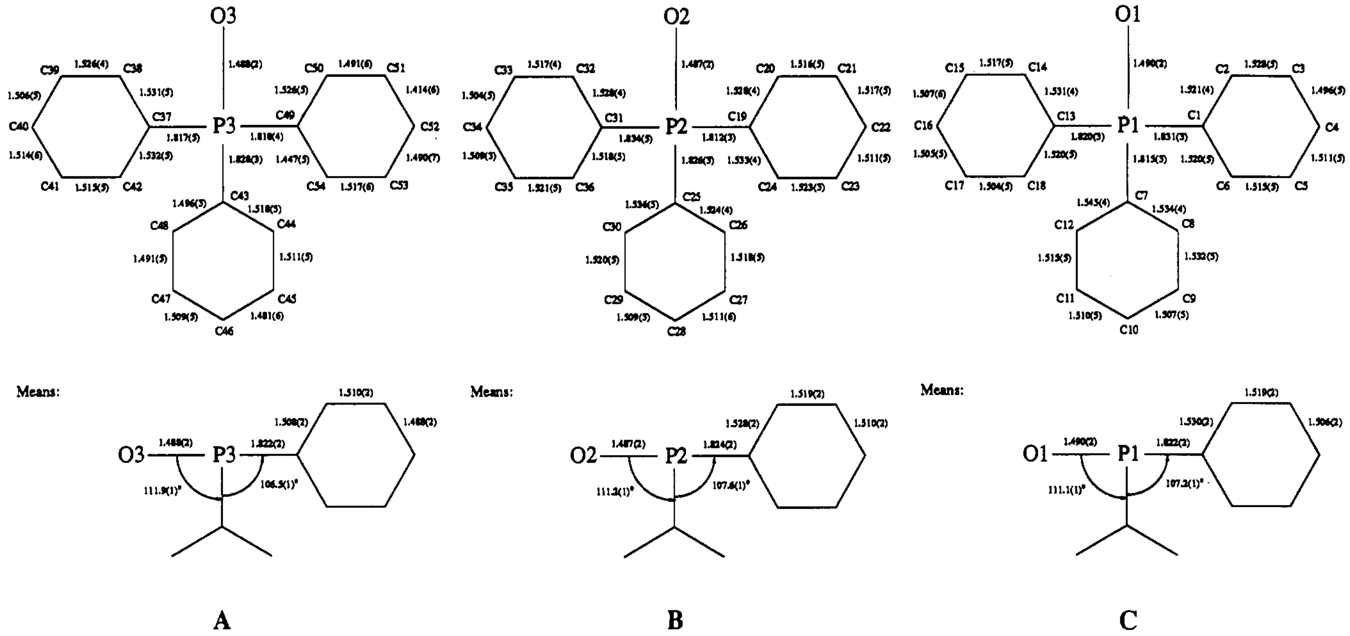

similar to the P–O bond lengths in the various polymorphs of Ph_3PO whose structures have been determined with varying degrees of accuracy.[16-20] Differences in molecular dimensions between Cy_3PO and Me_3PO appear exactly as anticipated considering the steric effects of the cyclohexyl groups.

We found that Cy_3PO crystallizes in the triclinic space group $P\bar{1}$ with $Z = 6$. Thus, the asymmetric unit contains three separate Cy_3PO molecules implying a maximum of three signals in the solid-state ^{31}P NMR spectrum. In fact, two signals in an approximately 2:1 intensity ratio were observed (Figure 2), and this ratio was confirmed by single-pulse experiments. Close inspection of the X-ray data (Table V) shows us that although two of the molecules in the asymmetric unit are well-behaved, one shows evidence of higher thermal motion of the cyclohexyl groups. Whether or not this minor difference is related to the differences seen in the solid-state NMR spectrum is unclear. Certainly this is not manifested in the line widths of the two signals (see Figure 2b), which are very similar. This similarity is further demonstrated by the experimentally indistinguishable values of T_{CP} (197 ± 10 and 221 ± 12 μs), $T_{1\rho}(^1H)$ (3.28 ± 0.18 and 3.34 ± 0.18 ms), and T_1 (^{31}P) (38 ± 1 and 39 ± 1 s) for the two types of nuclei. Further, the spinning sidebands shown in Figure 2b all appear in intensity ratios of 2:1, suggesting that the shift anisotropies of the two types of ^{31}P nuclei are very similar. However, when the individual P–C and C–C bond lengths in each of the molecules found in the asymmetric unit are averaged (see Chart I), it is perhaps still tempting to suggest that the NMR experiment can differentiate molecule A from B and C. Clearly, further examples of this phenomenon must be sought before it can be fully understood.[24]

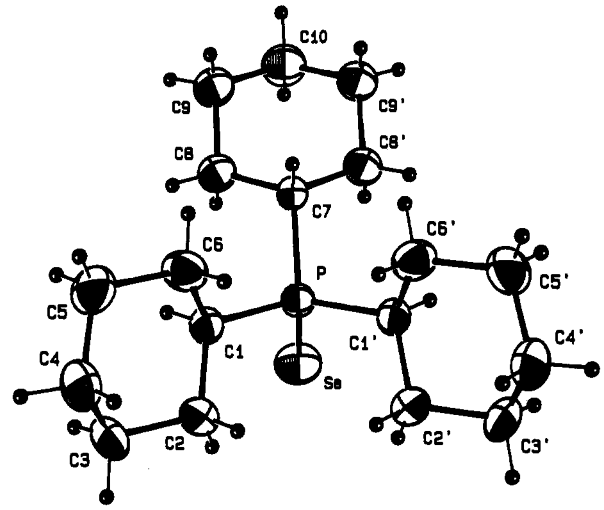

Figure 5. Molecular structure of $SePCy_3$, showing 50% probability ellipsoids.

Table VII. Positional Parameters and Equivalent Isotropic Displacement Parameters for $SePCy_3$ (3)

atom	x	y	z	$B/Å^{2\,a}$
Se	0.16463 (4)	0.250	0.55532 (5)	4.18 (1)
P	−0.02343 (9)	0.250	0.5280 (1)	2.44 (2)
C1	−0.0897 (3)	0.1528 (2)	0.5950 (3)	2.79 (6)
C2	−0.0672 (3)	0.1413 (2)	0.7386 (3)	3.46 (6)
C3	−0.0979 (3)	0.0505 (2)	0.7801 (3)	4.25 (8)
C4	−0.2266 (3)	0.0290 (2)	0.7459 (3)	4.64 (8)
C5	−0.2533 (4)	0.0444 (2)	0.6042 (3)	4.65 (8)
C6	−0.2204 (3)	0.1347 (2)	0.5634 (3)	3.80 (7)
C7	−0.0627 (4)	0.250	0.3556 (4)	2.53 (8)
C8	−0.0167 (3)	0.3295 (2)	0.2882 (3)	3.59 (7)
C9	−0.0464 (4)	0.3287 (2)	0.1445 (3)	4.31 (8)
C10	0.0009 (6)	0.250	0.0802 (4)	4.9 (1)

^{a} B values for anisotropically refined atoms are given in the form of the isotropic equivalent displacement parameter.

Unlike the oxide, tricyclohexylphosphine sulfide crystallizes in the orthorhombic system. The structure was refined and reported in the centrosymmetric space group *Pnma* although second

---

[24] Increase in the number of resonances as a result of crystallographic inequivalence has recently been observed by Harris et al. in the ^{13}C CP/MAS NMR spectrum of anhydrous androstanolone.[25] These workers, however, made no attempt to link a particular resonance with a given crystallographic site. Similar observations have also been made by Cheetham et al. in their ^{31}P MAS NMR studies of crystalline inorganic phosphates. These workers reported two methods that were successfully employed to assign ^{31}P resonances to particular phosphorus atoms in the asymmetric unit: The first method consists of making an analysis of the bonding around the phosphorus atoms and using an empirical relationship between bond strengths and chemical shifts to make the assignment.[26] The second method involves distinguishing between the resonances by inducing small local structural changes around the phosphorus atoms by cation substitution.[27]

[25] Harris, R. K.; Say, B. J.; Yeung, R. R.; Fletton, R. A.; Lancaster, R. W. *Spectrochim. Acta, Part A* **1989**, *45*, 465.

[26] Cheetham, A. K.; Clayden, N. J.; Dobson, C. M.; Jakeman, R. J. B. *J. Chem. Soc., Chem. Commun.* **1986**, 195.

[27] Jakeman, R. J. B.; Cheetham, A. K. *J. Am. Chem. Soc.* **1988**, *110*, 1140.

Table VIII. Selected Bond Lengths (Å) and Angles (deg) for $SePCy_3$ (3)[a]

Se–P	2.108 (1)	C2–C3	1.536 (5)
P–C1	1.839 (3)	C3–C4	1.513 (5)
P–C7	1.839 (4)	C4–C5	1.517 (5)
C1–C2	1.520 (4)	C5–C6	1.533 (5)
C1–C6	1.516 (4)		
Se–P–C1	110.2 (1)	C1–C2–C3	110.4 (2)
Se–P–C7	111.4 (1)	C2–C3–C4	110.8 (3)
C1–P–C1′	113.3 (1)	C3–C4–C5	112.0 (3)
C1–P–C7	105.8 (1)	C4–C5–C6	111.8 (3)
P–C1–C2	113.8 (2)	C1–C6–C5	110.1 (3)
P–C1–C6	117.3 (2)	P–C7–C8	111.4 (2)
C2–C1–C6	110.3 (2)		

[a] Numbers in parentheses are estimated standard deviations in the least significant digits.

harmonic generation established, without ambiguity, the absence of a center of inversion.[28] The correct space group was thus shown to be $Pn2_1a$ with $Z = 4$, although attempts to refine the data in this noncentrosymmetric space group were not satisfactory. For Cy_3PS we thus find that irrespective of the space group the asymmetric unit contains one crystallographically unique phosphorus, and so we expect only a single signal in the solid-state ^{31}P NMR spectrum, exactly as observed.

Tricyclohexylphosphine selenide exhibits a single signal in the solid-state ^{31}P NMR spectrum, with the expected $^{31}P-^{77}Se$ coupling, suggesting a closer relationship to Cy_3PS than to Cy_3PO. Since structural data were not available for this compound, we obtained single crystals and, after establishing that the recrystallized material still exhibited the spectrum shown in Figure 2, solved the structure (Figure 5). Crystal data are collected in Table II, while Table VII shows positional and equivalent isotropic displacement parameters. Selected bond lengths and angles are given in Table VIII. At the molecular level, the structure of Cy_3PSe shows the expected geometry about phosphorus and cyclohexyl groups with a chair conformation. The P–Se bond length of 2.108 (1) Å is comparable to that reported for Me_3PSe (2.111 (3) Å).[29]

We found that Cy_3PSe crystallizes in the orthorhombic system and that the data could be successfully refined in the centrosymmetric space group *Pnma* with $Z = 4$. Without an available, sensitive, and unambiguous test for the absence of a center of inversion, such as second harmonic generation, we have reported the data in the centrosymmetric space group. Indeed, the possible space group ambiguity encountered here is undetectable by solid-state ^{31}P NMR measurements. Thus, for the noncentrosymmetric space group $Pn2_1a$ with $Z = 4$, the asymmetric unit contains a single molecule. For the centrosymmetric space group *Pnma* with $Z = 4$, the asymmetric unit contains a half-molecule. In either case, we predict a single ^{31}P resonance in the solid-state NMR spectrum, exactly as observed. The possibility exists that this space group ambiguity could be probed by solid-state ^{13}C NMR measurements, since, in $Pn2_1a$, the asymmetric unit contains 18 unique carbon atoms but, in *Pnma*, the asymmetric unit contains only 8 carbon atoms plus 2 half-atoms. Thus, observation of signals representing more than 10 carbon centers would indicate the absence of a center of inversion. Clearly, Cy_3PSe is not the best compound to explore this situation, since there is the potential for coupling between ^{13}C and both ^{31}P and ^{77}Se that will unduly complicate the spectra. Nonetheless, as a test, we recorded the ^{13}C CP/MAS NMR spectra of both Cy_3PS and Cy_3PSe to see if they would provide useful space group information. Since signal overlap in the ^{13}C CP/MAS NMR spectra of Cy_3PS and Cy_3PSe was expected to be a problem, we first recorded their ^{13}C solution NMR spectra. The ^{13}C solution NMR data obtained for these two compounds are shown in Table IX. These indicate that the signals corresponding to C_2, C_3, and C_4 in both compounds will undoubtedly overlap in the solid-state spectra but that useful space group information might be obtained from the signals corresponding to the carbon atoms directly attached to phosphorus (δ = 37.01 ppm and δ = 36.47 ppm in Table IX). The ^{13}C CP/MAS NMR spectra of Cy_3PS and Cy_3PSe are shown in Figure 6. As expected, in both cases, the signals corresponding to the methylene carbons overlap and, consequently, no useful space group information can be obtained from these. On the other hand, the signals due to the carbon atoms directly attached to phosphorus are well separated from the rest of the spectrum. It is interesting to note that these signals are no longer observed around 37.0 ppm as in solution but have undergone a significant downfield shift to approximately 45.0 ppm; this phenomenon is a good illustration of the influence of medium effects on the magnetic environment of the nuclei. In the case where the correct space group is $Pn2_1a$, we expect the region corresponding to C_1 in the ^{13}C CP/MAS NMR spectra of both compounds to consist of a maximum of three doublets with approximately the same intensity (coupling between C_1 and ^{77}Se in the case of Cy_3PSe is not observed). On the other hand, in the case where the correct space group is *Pnma*, we expect the same region of the spectrum to display no more than two doublets in an approximately 2:1 ratio. The downfield region of the ^{13}C CP/MAS NMR spectrum of Cy_3PS actually displays one doublet at 45.1 ppm with $^1J(^{31}P,^{13}C) = 40$ Hz, and that of Cy_3PSe also displays one doublet at 44.6 ppm with $^1J(^{31}P,^{13}C) = 31$ Hz. These results therefore indicate that chemical shift differences between the three ($Pn2_1a$) or two (*Pnma*) crystallographically unique methine carbons in these two compounds must be below the resolution limit of the solid-state NMR experiment. Appropriate model compounds are currently being sought to explore the use of solid-state NMR methods in resolving these types of

Table IX. Solution $^{13}C\{^1H\}$ NMR Data[a]

	$SPCy_3$		$SePCy_3$[b]	
	δ/ppm	J(P,C)/Hz	δ/ppm	J(P,C)/Hz
C1	37.01	45	36.47	37
C2	27.23	3	27.98	3
C3	27.03	12	27.00	12
C4	26.06	0	26.04	0

[a] Measured in $CDCl_3$ at room temperature and referenced to internal $SiMe_4$. [b] No coupling between C1 and ^{77}Se was observed.

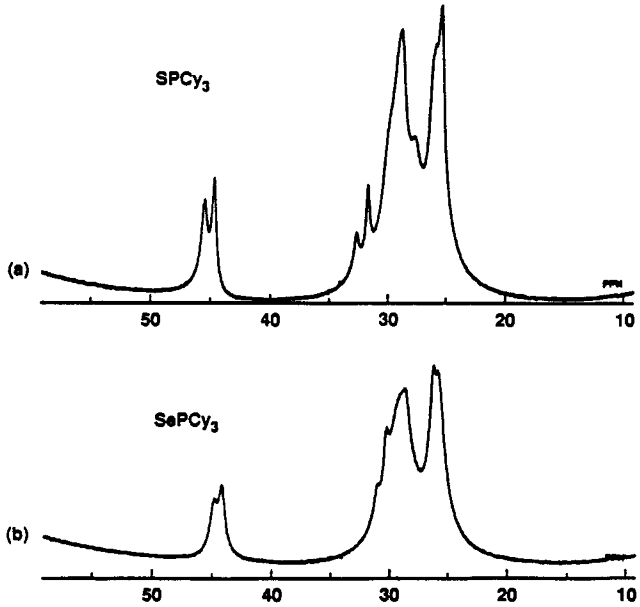

Figure 6. Solid-state ^{13}C NMR spectra: (a) $SPCy_3$, 3663 transients, 0 Hz line broadening, spinning rate = 4.7 kHz; (b) $SePCy_3$, 2538 transients, 0 Hz line broadening, spinning rate = 4.7 kHz.

---

(28) Kerr, K. A.; Boorman, P. M.; Misener, B. S.; Van Roode, J. G. H. *Can. J. Chem.* **1977**, *55*, 3081.

(29) Cogne, A.; Grand, A.; Laugier, J.; Robert, J. B.; Wiesenfeld, L. *J. Am. Chem. Soc.* **1980**, *102*, 2238.

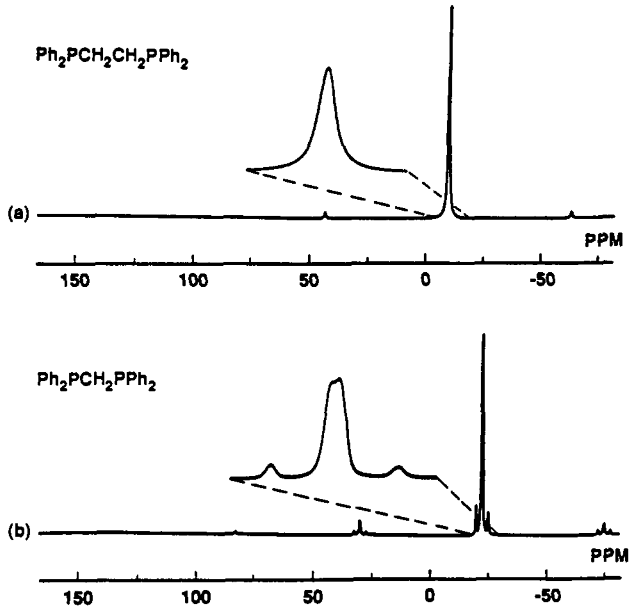

Figure 7. Solid-state ^{31}P NMR spectra: (a) $Ph_2PCH_2CH_2PPh_2$ (dppe), 6342 transients, 0 Hz line broadening, spinning rate = 4.3 kHz; (b) $Ph_2PCH_2PPh_2$ (dppm), 4997 transients, 0 Hz line broadening, spinning rate = 4.2 kHz.

crystallographic space group ambiguities.

Further information concerning solid-state effects on ^{31}P NMR spectra might be derived from examination of bis(tertiary phosphines) of the general type $R_2P(CH_2)_nPR_2$, where the possibility of ^{31}P–^{31}P coupling exists for materials in appropriate crystal systems. The observation of such coupling might be of use in differentiating intermolecular and intramolecular effects. Accordingly, we have examined $Ph_2P(CH_2)_2PPh_2$ (dppe) and $Ph_2PCH_2PPh_2$ (dppm). The X-ray structures of two polymorphs of dppe have been reported.[30] Both are in the monoclinic space group $P2_1/n$ with $Z = 2$, and the conformations of the molecules in the two polymorphs are said to be practically identical. The polymorphs differ only in the packing of these molecules, and each polymorph has a half-molecule per asymmetric unit. Thus, the solid-state ^{31}P NMR spectrum of either polymorph or, indeed, a mixture of polymorphs is anticipated to exhibit only a single resonance and one signal is in fact observed (Figure 7) in the spectrum of a commercial sample.

The solid-state ^{31}P NMR spectrum of dppm (Figure 7) proved to be most interesting, since it contains an apparent AB pattern implying coupling between crystallographically inequivalent ^{31}P nuclei within a dppm molecule.[31] The reported structure shows that dppm crystallizes in the orthorhombic space group *Pbca* with $Z = 8$.[32] The asymmetric unit thus contains one dppm molecule and hence two crystallographically inequivalent ^{31}P nuclei. Interestingly, the coupling between these crystallographically inequivalent nuclei of 210 Hz is significantly different from the value of +125 Hz measured for dppm in solution by $^{13}C\{^1H,^{31}P\}$ triple resonance.[33] This difference in the magnitudes of $^2J(^{31}P,^{31}P)$ in solution and in the solid state implies significant conformational differences for the dppm molecule. In a related study, Maciel et al.[3c] have reported the presence of two signals in the solid-state ^{31}P NMR spectrum of (*S*,*S*)-2,3-bis(diphenylphosphino)butane (chiraphos) but no coupling between the phosphorus centers was observed. The solution $^{31}P\{^1H\}$ NMR spectrum of chiraphos consists of only a single resonance.[3c]

Conclusions

The results presented here show that solid-state NMR spectroscopy and X-ray crystallography each provide information that is complementary. It has been demonstrated that X-ray crystallographic data can be successfully employed to determine the maximum number of signals observed in the solid-state CP/MAS NMR spectrum of a compound on the basis of the number of crystallographically unique nuclei present in its asymmetric unit. Furthermore, it has been shown that crystallographic inequivalence, although obviously necessary, is not sufficient for the observation of separate resonances and that the local environment of each crystallographically unique nucleus also has to be taken into consideration. Electron density measurements may prove useful in the study of such problems. Clearly, care must be exercised when solid-state NMR methods are used to resolve crystallographic space group ambiguities.

Acknowledgment. Thanks are expressed to the College of Arts and Sciences of the University of Toledo for use of the X-ray crystallographic facilities and to the Ohio Board of Regents for funding of the solid-state NMR spectrometer. We thank Dr. R. E. Wasylishen for helpful discussion.

Supplementary Material Available: For **1**–**3**, listings of experimental details, final hydrogen coordinates, anisotropic thermal parameters, bond lengths, and bond angles (26 pages); tables of structure factors (40 pages). Ordering information is given on any current masthead page.

---

(30) Pelizzi, C.; Pelizzi, G. *Acta Crystallogr., Sect. B* **1979**, *35*, 1785.

(31) Other AB patterns resulting from the coupling of crystallographically inequivalent nuclei present in a single molecule have also been observed in the ^{31}P CP/MAS NMR spectra of several diphosphine disulfides[7] and in the ^{31}P CP/MAS NMR spectrum of *trans*-$[PtI_2(P\{n\text{-}Bu\}_3)_2]$.[3w]

(32) Schmidbaur, H.; Reber, G.; Schier, A.; Wagner, F. E.; Müller, G. *Inorg. Chim. Acta* **1988**, *147*, 143.

(33) Colquhoun, I. J.; McFarlane, W. *J. Chem. Soc., Dalton Trans.* **1982**, 1915.